Macromolecules

Article

pubs.acs.org/Macromolecules

# Synthesis of Phosphate Buffered Saline- and Ascorbic Acid-Responsive Polymeric Nanocapsules with Cross-Linked Poly(2-hydroxyethyl methacrylate) and Polystyrene Blocks

Bing Huang, Shuxue Zhou, Min Chen, and Limin Wu*

Department of Materials Science and State Key Laboratory of Molecular Engineering of Polymers, the Advanced Coatings Research Center of MEC, Fudan University, Shanghai 200433, China

Supporting Information

**ABSTRACT:** Polymeric nanocapsules with cross-linked poly(2-hydroxyethyl methacrylate) and polystyrene blocks (PS-*b*-(*c*-PHEMA) nanocapsules) were synthesized via the surface-initiated atom transfer radical polymerization and atom transfer nitroxide radical coupling reactions. With alkoxyamine bonds as the cross-linkers, the nanocapsules exhibited unique responsive behavior: When PBS and oxygen existed, these nanocapsules were broken down into pieces, which self-assembled into nanocapsules again when ascorbic acid was added. When PBS, ascorbic acid, and oxygen existed together, these nanocapsules self-assembled into larger capsules. However, both the nanocapsules and capsules would finally disintegrate into pieces as the time extended.

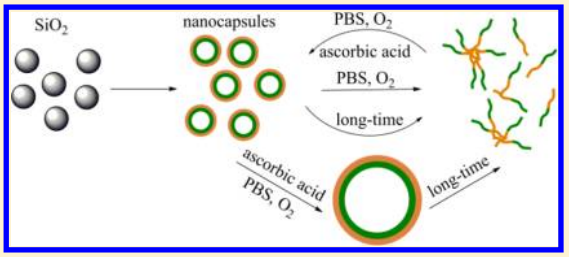


## INTRODUCTION

Functional polymeric nanocapsules are of particular interest due to their potential for the encapsulation of large quantities of guest molecules or large-sized guests within their empty core domain and higher mechanical and chemical stability than liposomes. These materials could be useful in applications in areas such as diverse delivery vesicles for drugs,[1] coatings,[2] protective shells for DNA, RNA, and functional enzymes,[3] self-healing materials,[4] and catalysts.[5]

Generally, there are four classical strategies for the fabrication of nanocapsules, including the self-assembly, the template, the emulsion/suspension polymerization, and the dendrimer approaches.[6−9] Compared with other methods, the template processes via the layer-by-layer technique or surface polymerization technique show the most efficiency in the precise controlling of the inner and the shell diameters and low size dispersibility of the nanocapsules.[10−12] The surface-initiated controlled/living radical polymerization (CLRP) technique also provides a means for the synthesis of nanocapsules with the controllable shell thickness.[13−16] Of course, the most challengeable topic is still the synthesis of intelligent polymeric nanocapsules.

Although a multitude of intelligent micelles and hollow spheres, which are sensitive to pH, temperatures, ions, and oxidation−reduction, have been designed and reported in recent years,[17−24] the intelligent nanocapsules which are responsive to phosphate buffered saline (PBS) and ascorbic acid are rarely reported to the best of our knowledge. PBS is one of the most commonly used biological buffers. It is isotonic and nontoxic to cells and has the ability to maintain their osmolarity. Ascorbic acid, one form of vitamin C, is a naturally occurring organic compound with antioxidant property and an essential nutrient for humans and other animal species. Thus, the possible nanocapsules sensitive to PBS and ascorbic acid could be used as an efficiently controlled delivery carrier.

In this study, we have successfully synthesized the polymeric nanocapsules with the cross-linked poly(2-hydroxyethyl methacrylate) (PHEMA) and polystyrene (PS) blocks via the surface-initiated atom transfer radical polymerization and atom transfer nitroxide radical coupling reactions. With alkoxyamine bonds as the cross-linkers, the nanocapsules exhibit an unique responsive behavior to PBS and ascorbic acid: In the PBS solution at 37 °C and atmosphere, these nanocapsules are broken down into polymeric pieces, which self-assemble into nanocapsules again when ascorbic acid is added. In the mixture of PBS and ascorbic acid, the nanocapsules self-assemble into larger capsules. However, both the nanocapsules and capsules would finally disintegrate into polymeric pieces as the time extends.

## EXPERIMENTAL SECTION

**Materials.** Two kinds of monodisperse silica nanoparticles (SN) with diameters of 110 and 250 nm were synthesized according to the Stöber method.[25] All these silica particles were washed with ethanol and deionized water three times and then dried in a vacuum at 50 °C for 48 h before use. γ-Aminopropyltriethoxysilane (APTES) was bought from Shanghai Huarong Chemical Industrial Co. Ltd. and used as received. Styrene (St, 99%) and 2-hydroxyethyl methacrylate (HEMA, 96%) were received from Sinopharm Chemical Reagent Co. (SCR) and Aladdin Industrial Inc., respectively, and purified by passing the monomers through a column filled with basic alumina to remove the inhibitors. Tetrahydrofuran (THF, 99%, SCR) was refluxed and distilled from sodium naphthalenide solution. Copper(I)

Received: January 1, 2014
Revised: February 25, 2014
Published: March 6, 2014

  

Scheme 1. Synthetic Illustration of PS-*b*-(*c*-PHEMA) Nanocapsules

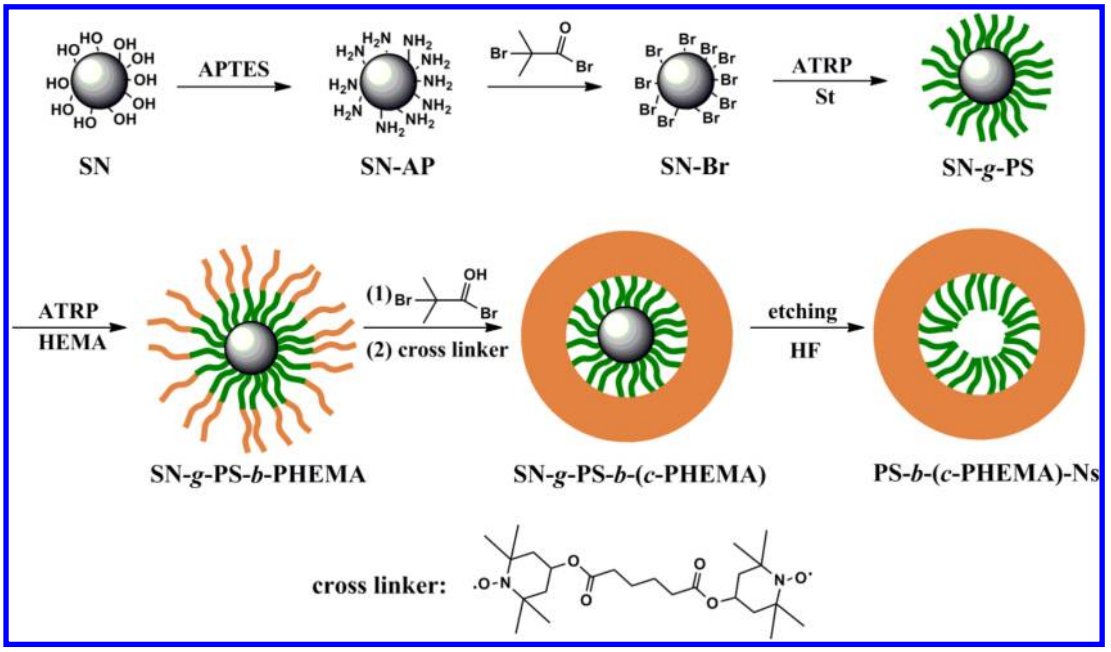


bromide (Cu(I)Br, 95%, SCR) and cuprous(I) chloride (Cu(I)Cl, 97%, SCR) were stirred overnight in acetic acid, filtered, then washed with ethanol and ethyl ether successively, and dried in a vacuum. 4-Hydroxyl-2,2,6,6-tetramethylpiperidine-1-oxyl (4-hydroxy-TEMPO) synthesized according to the literature[26] was purified by recrystallization with hexane. 2,2′-Bipyridine (bpy, 97%), 2-bromoisobutyryl bromide (99%), adipoyl chloride (99%), ascorbic acid (99%) and *N*,*N*,*N*′,*N*″,*N*‴-pentamethyldiethylenetriamine (PMDETA, 99%) were all purchased from Aldrich and used as received. Pyridine (99%), toluene (99%), hydrofluoric acid (HF, 40%), and other reagents were all purchased from SCR and used as received.

**Synthesis of Di[4-(2,2,6,6-tetramethylpiperidine-1-oxyl)] Adipate (*d*-HTEPMO).** The synthesis of *d*-HTEPMO was performed as follows:[27] a 250 mL oven-dried flask was charged with 4-hydroxy-TEMPO (10.3 g, 60 mmol) and purged with nitrogen for 30 min, followed by addition of anhydrous dichloromethane (70 mL) and pyridine (4.9 mL, 60 mmol). The flask was placed in an ice bath for 10 min and then added dropwise by a solution of adipoyl chloride (2.9 mL, 20 mmol) in 15 mL of anhydrous dichloromethane. The mixture was stirred at 0 °C for 1 h and then at room temperature for another 12 h. This solution was then washed several times with acidic water (pH 4). The organic phase was dried over magnesium sulfate and concentrated by rotary evaporation. The raw product was then purified by flash chromatography eluting with cyclohexane/ethyl acetate (8/2, gradually increasing to 5/5) to afford 8.4 g of red solid.

**Immobilization of Initiator on Silica Nanoparticles (SN-Br).** Silica particles were first functionalized by aminopropyl groups through the self-assembly of APTES from the surfaces of SN with the same procedures as reported previously,[28] to obtain aminopropyl-modified silica nanoparticles (SN-AP).

SN-AP (2.0 g) was dried by azeotropic distillation with toluene and then dispersed in 50 mL of anhydrous pyridine, to which 2.0 mL (16.0 mmol) of 2-bromoisobutyryl bromide was added dropwise at 0 °C within 30 min. After the reaction was allowed to proceed for 48.0 h, the SN-Br was centrifuged, washed with THF and ethanol thoroughly, and then dried under vacuum at 50 °C for the subsequent polymerization.

**Polystyrene Grafted Silica Nanoparticles (SN-*g*-PS).** 0.5 g of SN-Br, Cu(I)Br (0.288 g, 2.0 mmol), PMDETA (0.4 mL, 2.0 mmol), toluene (5.0 mL), and St (10.0 mL, 68 mmol) were added into a 100 mL dried ampule. The reaction mixture was degassed by three freeze–pump–thaw cycles and purged with nitrogen. The ampule was immersed in an oil bath maintained at 90 °C prior to polymerization. After polymerization reaction for different times, the ampule was dipped in liquid nitrogen to stop the polymerization. The products were separated by centrifugation, subjected to intense washing by THF and ethanol in combination with ultrasonication, and then dried under vacuum at 50 °C.

**Poly(2-hydroxyethyl methacrylate) Grafted SN-*g*-PS (SN-*g*-PS-*b*-PHEMA).** The mixture of SN-*g*-PS (0.3 g), bpy (0.31 g, 2.0 mmol), 2-butanone (12.0 mL), *n*-propanol (5.0 mL), and HEMA (5.0 mL) was added into a 100 mL dried ampule and degassed by three freeze–pump–thaw cycles. Then the Cu(I)Cl (0.10 g, 1.0 mmol) was added into the ampule under nitrogen as quickly as possible, followed by another three freeze–pump–thaw cycles. After being sealed under nitrogen, the ampule was immersed into an oil bath at 60 °C for polymerization reaction with different times and then taken out from the oil bath and dipped in liquid nitrogen to stop the polymerization. The products were separated by centrifugation, subjected to intense washing by THF and ethanol in combination with ultrasonication, and then dried under vacuum at 50 °C to obtain SN-*g*-PS-*b*-PHEMA.

**Cross-Linking of the PHEMA Shells.** The PHEMA shells were cross-linked via atom transfer nitroxide radical coupling reaction. The hydroxyl groups of SN-*g*-PS-*b*-PHEMA were modified into bromoisobutyryl groups using the similar procedures to the immobilization of initiator on silica nanoparticles. Then, the bromoisobutyryl-modified SN-*g*-PS-*b*-PHEMA (0.3 g), Cu(I)Br (0.029 g, 0.2 mmol), PMDETA (0.04 mL, 0.2 mmol), and toluene (5.0 mL) were added into a 100 mL dried ampule. This mixture was degassed by three freeze–pump–thaw cycles and purged with nitrogen, immersed in an oil bath at 90 °C for 12.0 h, and then dipped in liquid nitrogen to stop the polymerization. The products were separated by centrifugation and subjected to intense washing by THF and ethanol in combination with ultrasonication to obtain the cross-linked nanospheres (SN-*g*-PS-*b*-(*c*-PHEMA)).

**Etching of the Silica Templates.** The SN-*g*-PS-*b*-(*c*-PHEMA) (0.3 g) was added into 2 mL of 24% HF aqueous solution and stirred at room temperature for 2 h. The nanoparticles were collected by centrifugation and then dispersed in water (10 mL) and centrifuged. This washing procedure was repeated three times and then dried under vacuum at 50 °C for 24 h to obtain PS-*b*-(*c*-PHEMA) nanocapsules.

**PBS- and Ascorbic Acid-Responsive Nanocapsules.** The PS-*b*-(*c*-PHEMA) nanocapsules (1.0 mg) were dispersed in PBS solution (0.10 mol/L, 50 mL). The mixture was stirred at 37 °C in atmosphere (e.g., under oxygen condition) with or without ascorbic acid (1.0 mg).


dx.doi.org/10.1021/ma500006j | *Macromolecules* 2014, 47, 1914–1921

The sample was taken out at different intervals times and washed by water and ethanol to remove phosphate. The control experiment was carried out as follows. PS-*b*-(*c*-PHEMA) nanocapsules (1.0 mg), PBS solution (0.10 mol/L, 50 mL), and ascorbic acid (1.0 mg) were added into a 100 mL dried ampule, degassed by three freeze−pump−thaw cycles, and purged with nitrogen (e.g., under nitrogen condition). The mixture was stirred at 37 °C for 24.0 h, then separated by centrifugation, and washed by water and ethanol. Another nanocapsule (1.0 mg) was added into 50 mL water, then mixed with ascorbic acid (1.0 mg), and stirred at 37 °C for 24.0 h.

**Measurements.** Gel permeation chromatographic (GPC) analysis of PS was performed in THF at 35 °C with an elution rate of 1.0 mL/min on an Agilent 1100 equipped with a G1310A pump, a G1362A refractive index detector, and a G1314A variable wavelength detector. One 5 $\mu$m LP gel column (500 Å, molecular range 500−2 × $10^4$ g/mol) and two 5 $\mu$m LP gel mixed bed column (molecular range 200−3 × $10^6$ g/mol) were calibrated by PS standard samples. The injection volume was 20 $\mu$L, and the concentration was 5 mg/mL. $^1$H NMR spectra were recorded on a DMX 500 MHz spectrometer in $CDCl_3$ and DMSO-$d_6$ with tetramethylsilane (TMS) as the internal reference for chemical shifts. The purified and dried samples were subjected to thermogravimetric analysis under air using a Pyris 1 TGA instrument at a heating rate of 20 °C $min^{-1}$ from 120 to 800 °C. Transmission electron microscopy (TEM) images were taken with a Philips CM200FEG field emission microscope. For the TEM observations, samples were dispersed in ethanol and then dried on a holey carbon film Cu grid. All dynamic light scattering (DLS) experiments were carried out at 25 °C on a Malvern particle size analyzer (Model Zetasizer NANO ZS90). In all cases, nanoparticles (~0.01 mg) dispersed in ethanol (1 mL) were measured at a scattering angle of 90°.

## RESULTS AND DISCUSSION

Scheme 1 briefly describes the synthetic procedures of nanocapsules. First, bromo groups were located on the surfaces of silica nanoparticles by ammonification and esterification. Next, the PS-*b*-PHEMA polymer chains were grafted from silica nanoparticles via surface-initiated atom transfer radical polymerization. This procedure yielded core−shell microparticles with silica core and outer layer of covalently attached, well-defined uniform thickness block copolymers. Then, the hydroxyl groups of PHEMA blocks were modified into the bromoisobutyryl groups, which were further cross-linked by atom transfer nitroxide radical coupling reaction. Finally, the silica cores were etched by HF to produce polymeric nanocapsules.

**Synthesis of Initiator-Functionalized Silica Templates.** Figure 1a shows a typical TEM image of monodisperse $SiO_2$ solid spheres of 250 nm ($SN_1$) in diameter prepared by the well-known Stöber process. Table 1 reveals that the diameters

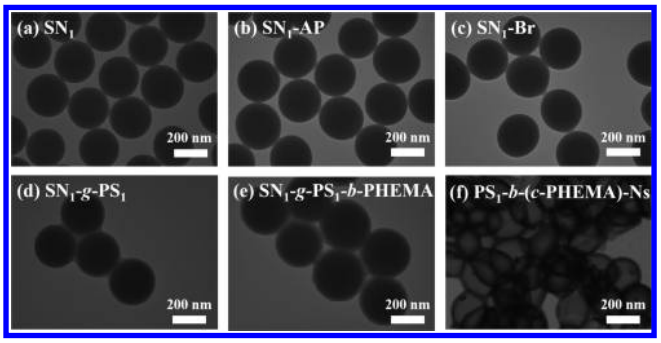


**Figure 1.** TEM images of the nanospheres and nanocapsule at different stages.

($D_{TEM}$) and hydrodynamic diameters ($D_h$) of all the silica nanoparticles and the corresponding polymer-grafted nanoparticles and polymeric nanocapsules. After being modified by aminopropyl and then bromo groups, their mean size and size distribution did not vary (Figure 1b,c). TGA analysis displays that the noticeable weight loss of the pure $SiO_2$ was 9.50% and occurred between 120 and 800 °C due to the elimination of physisorbed water or adsorbed gases (Figure 2A), while the weight losses of $SN_1$-AP and $SN_1$-Br were 9.67% and 10.76%, respectively (Figure 2B,C). Based on these data and eq 1[29]

$$G_1 = \frac{\frac{W\%_{\text{initiator+silica}}}{100 - W\%_{\text{initiator+silica}}} - \frac{W\%_{\text{silica}}}{100 - W\%_{\text{silica}}}}{M_{\text{initiator}} \times S_{\text{sp}}} \times N_A \ (\text{groups/nm}^2) \quad (1)$$

where $W\%_{\text{initiator+silica}}$ is the weight loss percentage after initiator grafting, $W\%_{\text{silica}}$ is the weight loss percentage corresponding to the weight loss of SN-AP, $N_A$ is Avogadro's number, $M_{\text{initiator}}$ is the molar mass of the initiator calculated by subtracting the molar mass of the Br atoms ($M_{\text{initiator}}$ = 150 g/mol), and $S_{sp}$ is the specific surface area of silica microsphere (which is 12.6 and 28.7 $m^2$/g, corresponding to silica nanoparticles with diameters of 250 nm ($SN_1$) and 110 nm ($SN_2$), respectively). Thus, the initiator grafting density of $SN_1$-Br was calculated to be 4.3 groups/$nm^2$.

**Polystyrene Grafted Silica Nanoparticles (SN-*g*-PS).** The PS grafted on the surfaces of silica nanoparticles was carried out by the surface-initiated atom transfer radical polymerization of styrene from the surfaces of the 2-bromopropionamide-functionalized silica nanoparticles. By controlling the reaction time, a series of PS brushes with different number-average molecule weight ($M_n$) were obtained. In order to measure the molecule weight by GPC, the as-obtained SN-*g*-PS was dissolved in HF to remove silica and then precipitated in $CH_3OH$. Figure 3 presents the GPC traces ($PS_1$ to $PS_4$). With the increase in polymerization time from 4 to 12 h, the $M_n$ increased from 1.5 × $10^4$ to 15 × $10^4$ g/mol although different sizes of silica nanoparticles were used, as shown in Table 2.

The TGA thermogram of $SN_1$-*g*-$PS_1$ shows a significant weight loss (Figure 2D) about 27.8%. According to eq 2

$$G_{PS} = \frac{\frac{W\%_{\text{PS+silica}}}{100 - W\%_{\text{PS+silica}}} - \frac{W\%_{\text{initiator+silica}}}{100 - W\%_{\text{initiator+silica}}}}{M_{n(\text{GPC})} \times S_{sp}} \times N_A \ (\text{polymer chains/nm}^2) \quad (2)$$

where the $W\%_{\text{polymer+silica}}$ is the weight loss percentage after polymerization and $M_{n(GPC)}$ is the experimental molar mass of the grafted polymer chains. The polymer grafting density of $SN_1$-*g*-$PS_1$ was calculated to be 0.16 polymer chains/$nm^2$, which is less than the initiator grafting density of $SN_1$-Br. Similar results can also be obtained by the TGA thermograms of other types of SN-*g*-PS as shown in Figure S1 of the Supporting Information. This suggests that some of the initiators on the silica remained intact during polymerization owing to the steric effect.

Figure 1d shows the as-obtained $SN_1$-*g*-$PS_1$ nanospheres have core−shell structure and 276 nm in mean diameter. The thickness of the PS shell is dependent upon the $M_n$ of PS. Figure 4A reveals the $D_h$ distribution of $SN_1$-*g*-$PS_1$. Compared to that of $SN_1$, the mean $D_h$ increased from 294 to 333 nm, which should be attributed to the grafted PS.

**Table 1. Physical Parameters of Different Nanospheres**

| samples | $D_{TEM}$[a] (nm) | $D_h$[b] (nm) | PDI[c] | samples | $D_{TEM}$[a] (nm) | $D_h$[b] (nm) | PDI[c] |
|---|---|---|---|---|---|---|---|
| $SN_1$ | 234−259 | 294 | 0.097 | $SN_1$-*g*-$PS_2$-*b*-PHEMA | 325−361 | 581 | 0.64 |
| $SN_2$ | 112−150 | 180 | 0.085 | $SN_2$-*g*-$PS_3$-*b*-PHEMA | 197−223 | 341 | 0.48 |
| $SN_1$-*g*-$PS_1$ | 274−278 | 333 | 0.18 | $SN_2$-*g*-$PS_4$-*b*-PHEMA | 262−283 | 396 | 0.40 |
| $SN_1$-*g*-$PS_2$ | 289−302 | 364 | 0.12 | $PS_1$-*b*-(*c*-PHEMA)-Ns | 231−253 | 925 | 0.68 |
| $SN_2$-*g*-$PS_3$ | 130−164 | 230 | 0.45 | $PS_2$-*b*-(*c*-PHEMA)-Ns | 235−261 | 955 | 0.71 |
| $SN_2$-*g*-$PS_4$ | 184−215 | 255 | 0.36 | $PS_3$-*b*-(*c*-PHEMA)-Ns | 61−74 | 287 | 0.69 |
| $SN_1$-*g*-$PS_1$-*b*-PHEMA | 303−333 | 570 | 0.38 | $PS_4$-*b*-(*c*-PHEMA)-Ns | 70−83 | 319 | 0.53 |

[a]By TEM. [b]By DLS. [c]By DLS.

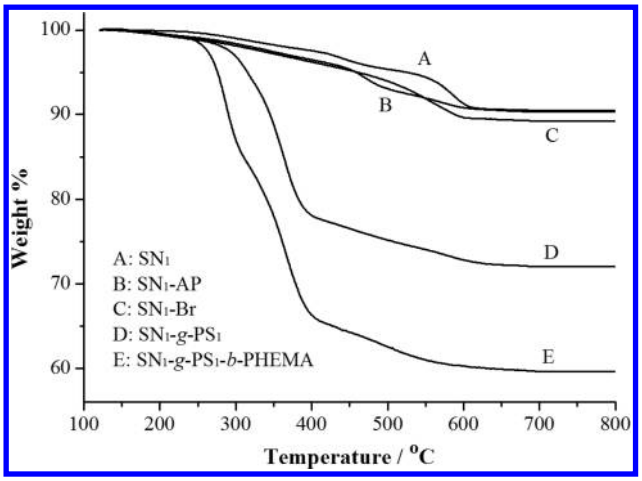


**Figure 2.** TGA thermograms of the nanospheres and nanocapsule at different stages.

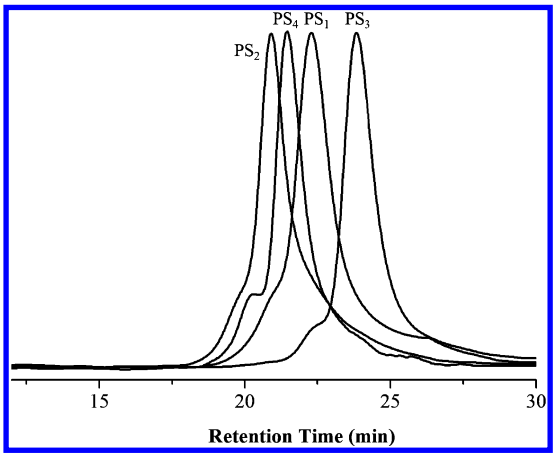


**Figure 3.** GPC profiles of $PS_1$ ($M_n$ = 8 × $10^4$ g/mol), $PS_2$ ($M_n$ = 15 × $10^4$ g/mol), $PS_3$ ($M_n$ = 1.5 × $10^4$ g/mol), and $PS_4$ ($M_n$ = 12 × $10^4$ g/mol) with the reaction time for 8, 12, 4, and 10 h, respectively.

Figure 5A demonstrates the $^1$H NMR spectrum of PS chains cleaved from silica nanoparticles. The peaks at 6.27−7.22 ppm are attributed to the phenyl-ring protons of styrene units, further confirming that polystyrene brushes have been successfully grafted from the surfaces of the silica nanoparticles.

**PHEMA Grafted on the Surfaces of SN-*g*-PS Nanospheres.** The TGA thermogram of the as-obtained $SN_1$-*g*-$PS_1$-*b*-PHEMA nanospheres shows a significantly higher weight loss than $SN_1$-*g*-$PS_1$ nanospheres (Figure 2E). The $M_n$ of PHEMA block could be calculated to be 7.8 × $10^4$ g/mol based on eq 2. From the TEM images, the mean size increased to 343 nm and the shell thickness increased to 34 nm from the 13 nm of $SN_1$-*g*-$PS_1$ (Figure 1e and Table 1). The mean $D_h$ increased significantly due to the PHEMA blocks (Figure 4A).

**Table 2. Molecular Characterization Data for Different Polymers Obtained by Surface-Initiated ATRP**

| sample | $M_{n(PS),GPC}$[a] (g/mol) | PDI | $M_{n(PHEMA),TGA}$[b] (g/mol) | polymer chains/nm$^2$ [c] |
|---|---|---|---|---|
| $SN_1$-*g*-$PS_1$-*b*-PHEMA | 8 × $10^4$ | 1.10 | 7.8 × $10^4$ | 0.16 |
| $SN_1$-*g*-$PS_2$-*b*-PHEMA | 15 × $10^4$ | 1.09 | 9 × $10^4$ | 0.19 |
| $SN_2$-*g*-$PS_3$-*b*-PHEMA | 1.5 × $10^4$ | 1.11 | 5 × $10^4$ | 0.21 |
| $SN_2$-*g*-$PS_4$-*b*-PHEMA | 12 × $10^4$ | 1.12 | 8 × $10^4$ | 0.23 |

[a]By GPC. [b]The molecular weights of PHEMA were calculated according to TGA using eq 2. [c]Calculation according to TGA using eq 1.

The successful preparation of SN-*g*-PS-*b*-PHEMA nanospheres can also be confirmed by the $^1$H NMR spectrum of the $PS_1$-*b*-PHEMA block copolymers cleaved from the silica surfaces (Figure 5B), in which chemical shifts at 3.58 and 3.9 ppm (attributable to $-CH_2-OH$ and $-COOCH_2-$ groups of the PHEMA block, respectively) appear.

**Formation of the Polymeric Nanocapsules.** To obtain PBS- and ascorbic acid-responsive nanocapsules, alkoxyamine was used as the cross-linker. The alkoxyamine bonds were generated by atom transfer nitroxide radical coupling between bromo groups and 2,2,6,6-tetramethylpiperidinyl-1-oxy (TEMPO) groups. The bromo groups were formed by modifying the hydroxyl groups of PHEMA with 2-bromoisobutyryl bromide. The $^1$H NMR spectrum of the as-obtained $PS_1$-*b*-PHEMA-Br is shown in Figure 4C. Compared with the $^1$H NMR spectrum of $PS_1$-*b*-PHEMA, the chemical peaks at 3.58 and 3.90 ppm shifted to 4.13 and 4.33 ppm for $PS_1$-*b*-PHEMA-Br, indicating that the esterification reaction has been performed completely.

The nanocapsules (PS-*b*-(*c*-PHEMA)) were obtained by etching the silica templates of the cross-linked SN-*g*-PS-*b*-PHEMA nanospheres in an aqueous solution of HF. The hollow structure of the as-obtained $PS_1$-*b*-(*c*-PHEMA)-Ns is obviously observed by the TEM image (Figure 1f). The inner diameter of capsules was 180−245 nm, which was a little smaller than that of silica particles (250 nm) due to the osmotic pressure between the inner and outer of the capsules and the hydrophobic of PS block in ethanol. The nanocapsules with different sizes and PS-*b*-PHEMA molecular weights displayed the same character as indicated by Figure S2a−c. The $D_h$ of $PS_1$-*b*-(*c*-PHEMA)-Ns (Figure 4B) characterized by DLS was 925 nm, which was much larger than $D_{TEM}$. This may be owing to the aggregation of the nanocapsules in suspension.


dx.doi.org/10.1021/ma500006j | Macromolecules 2014, 47, 1914−1921

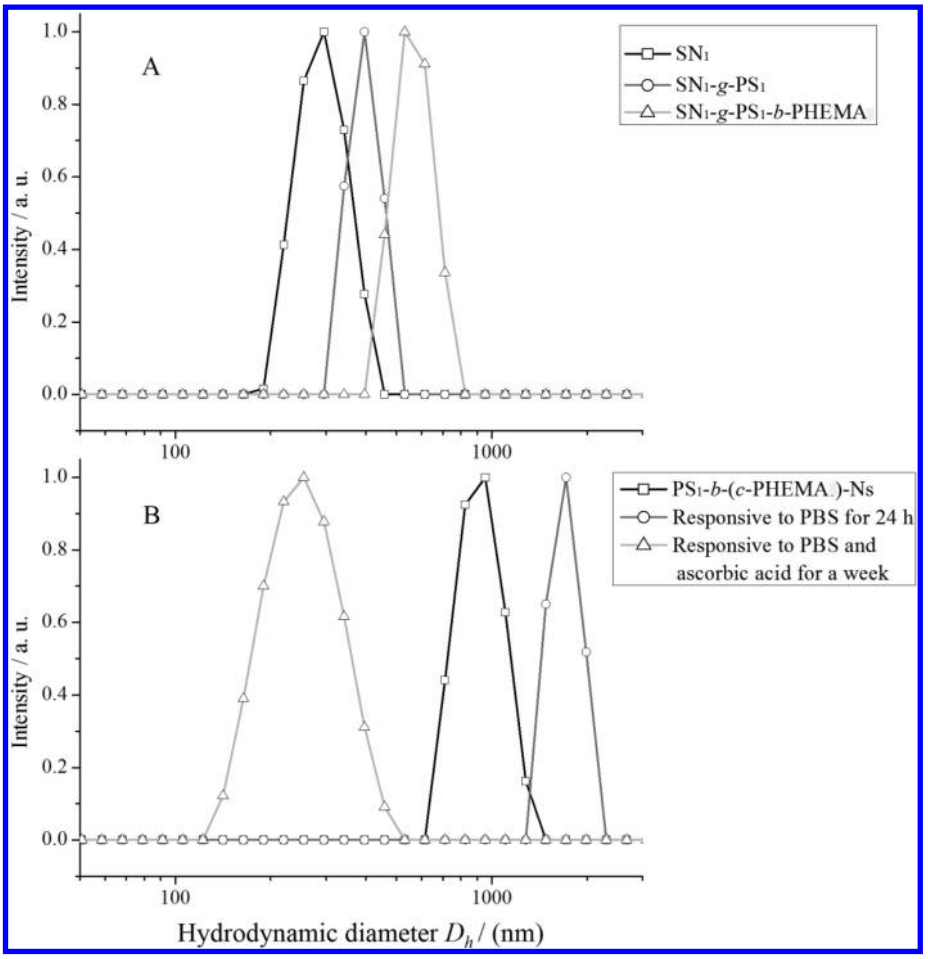


**Figure 4.** Distributions of hydrodynamic diameter $D_h$ of the nanospheres and nanocapsules at different stages.

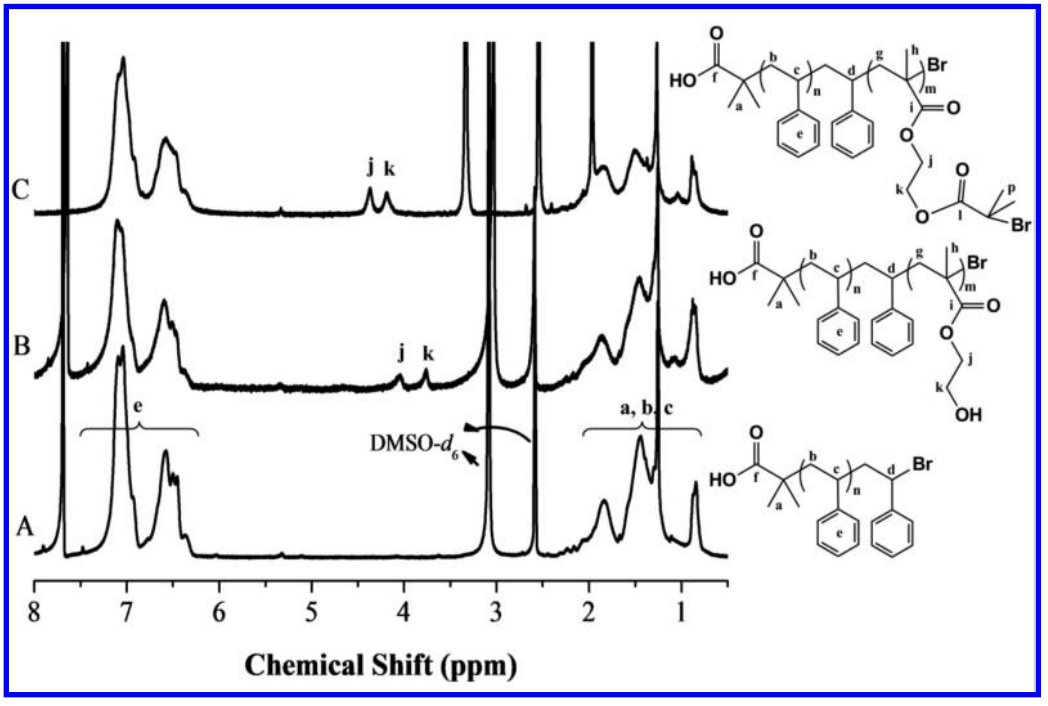


**Figure 5.** $^1$H NMR spectra of PS (A), PS-*b*-PHEMA (B), PS-*b*-PHEMA-Br (C), and PS-*b*-(*c*-PHEMA) nanocapsules (D) in $CDCl_3$ and DMSO-$d_6$.

**PBS- and Ascorbic Acid-Responsive Behaviors of the Nanocapsules.** In fact, the alkoxyamine bonds have been reported to have sensitivity to heat and ascorbic acid in multisegmented polymers.[27,30] Herein, we designed the original


dx.doi.org/10.1021/ma500006j | *Macromolecules* 2014, 47, 1914−1921

experiment to observe the responsive behaviors of PS-*b*-(*c*-PHEMA) nanocapsules to the most commonly used *in vitro* biological environment (PBS buffer solution, 37 °C and atmosphere). It is very interesting to see that the nanocapsules dispersed in PBS and ascorbic acid medium and stirred at 37 °C exhibited a special morphological evolution, as shown in Scheme 2. The original nanocapsules have the mean diameter

**Scheme 2. Schematic Illustration of the Nanocapsules Responding to PBS and Ascorbic Acid**

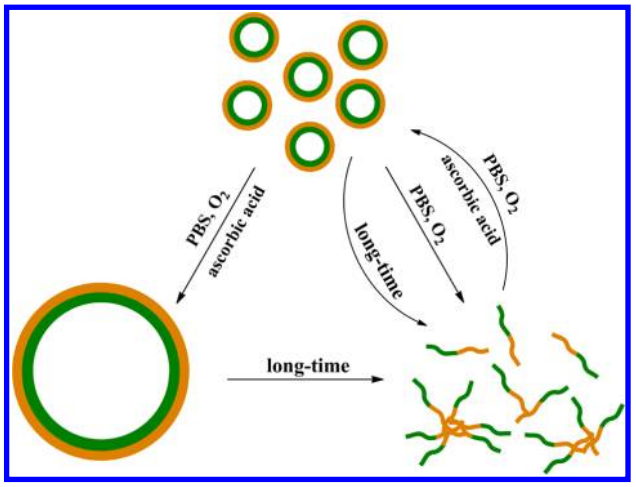


of 213 nm based on TEM image (Figure 1f). After being stirred for 12 h, the collapsing but size-comparable nanocapsules were observed (Figure 6a). After 24 h, much larger capsules, with the particle size distribution from 300 nm to 2 $\mu$m, were obtained (Figure 6b). These new large capsules were dispersed in the medium very well, and the shell thickness was thinner than that of original nanocapsules. When this solution was stirred for much longer time such as a week, all large capsules broke down into pieces (Figure 6c). Without ascorbic acid, all these nanocapsules directly disintegrated into pieces after 24 h (Figure 6d). Even if the reaction time increased, no nanocapsules were found. When ascorbic acid was added into this system, similar morphology to Figure 6a was seen after 12 h. When the nanocapsules were dispersed in ascorbic acid solution without PBS, no change in morphology was observed for these nanocapsules. Similar behavior was also found with much smaller size of nanocapsules as shown in Figure S2d–f. All these morphological evolutions suggest that PBS can accelerate the fragmentation reaction of the cross-linked bonds, while ascorbic acid can promote the addition reaction to form the cross-linked bonds.

Based on these experiments, the mechanism that the as-obtained PS-*b*-(*c*-PHEMA) nanocapsules responsive to PBS and ascorbic acid can be proposed as shown in Scheme 3. When the nanocapsules were stirred in PBS solution at 37 °C and atmosphere (e.g., under oxygen condition), the alkoxyamine bonds were slowly cleaved into carbon radicals and TEMPO radicals through the interaction of alkoxyamine and PBS because the rate constant $k_d$ for the alkoxyamine bond homolysis was subject to solvent and protonation effects of PBS.[31,32] It was found that with the increase in polarity of solvent, the rate constant became higher.[33] The protonated alkoxyamine even had a 20-fold increase in the rate constant compared to the nonprotonated homologue.[34] Without ascorbic acid, the TEMPO radicals were stable. But the carbon radicals were depleted by oxygen, so no new cross-linked bonds were formed. As a result, the nanocapsules disintegrated into some pieces with random cross-linked network structure after mixed for 24 h, as shown in Figure 6d. The DLS spectrum in Figure 4B displays that the hydrodynamic diameter of these pieces increased to 1700 nm, further proving the structure observed by TEM. When ascorbic acid was added into this system, the cleavage of alkoxyamine bonds continued, but the forming TEMPO radicals were easily reduced into TEMPOH by ascorbic acid.[35,36] However, under oxygen condition, these TEMPOH changed back to TEMPO radicals drastically.[37] With

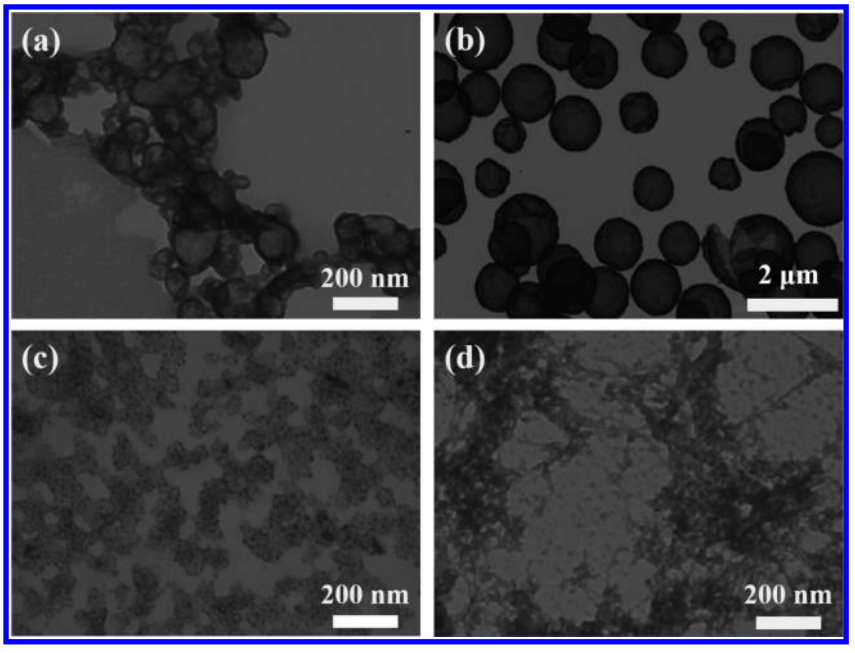


**Figure 6.** TEM images of nanocapsules responsive to PBS and ascorbic acid after 12 h (a), 24 h (b), a week (c), and the nanocapsules responsive to PBS without ascorbic acid for 24 h (d).


dx.doi.org/10.1021/ma500006j | *Macromolecules* 2014, 47, 1914–1921

Scheme 3. Responsive Mechanism of PS-*b*-(*c*-PHEMA) Nanocapsules to PBS and Ascorbic Acid

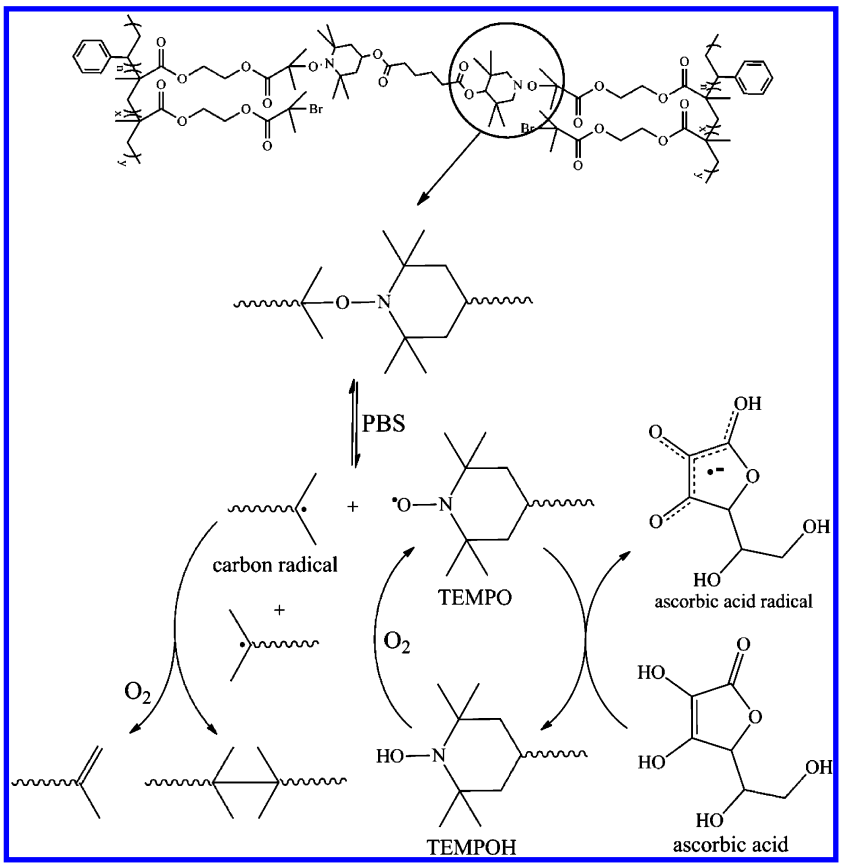


the consumption of oxygen, carbon radicals could be remained. Thus, the TEMPO radicals reacted with carbon radicals to generate cross-linked bonds again, and carbon radicals also reacted with each other via radical−radical coupling to produce stable carbon−carbon bonds. Because TEMPO tends to reside in the surface zones of the particles,[38,39] and the adsorbed ascorbic acid on the particles is prone to locate at the particle surfaces,[40] these PS-*b*-PHEMA blocks self-assembled into nanocapsules (similar to Figure 6a) again due to the reversible addition and fragmentation reactions on the surfaces of the particles. However, as the carbon radicals were finally exhausted by oxygen, the addition reaction would stop after 48 h. Finally, all these alkoxyamine bonds were cleaved, leaving ahead the cross-linked carbon−carbon bonds, as shown by only polymeric pieces not nanocapsules (Figure 6c). Figure 4B shows the mean $D_h$ shrank to 250 nm after time expending, also indicating that the most cross-linked bonds were cleaved, only polymeric pieces were obtained.

When the nanocapsules were stirred in PBS and ascorbic acid solution at 37 °C and atmosphere, the original PS-*b*-(*c*-PHEMA) nanocapsules self-assembled into large aggregates owing to the intermolecular and internanoparticles interactions. As the oxygen in solution was consumed gradually by the reversible transition of TEMPO and TEMPOH, the oxygen from atmosphere was dissolved into the solution again. The nanocapsules at the outer layer of the aggregates had the priority to get these dissolving oxygen molecules, producing reversible addition and fragmentation and radical−radical coupling reactions at the surfaces of aggregates. However, as the nanocapsules at the cores of the aggregates consumed the oxygen around, TEMPOH could not transition to TEMPO, resulting in the termination of the addition reaction between carbon radicals and TEMPO radicals. Thus, these nanocapsules at the cores collapsed, and the nanocapsules at the outer layers merged together with the thinning shells. Of course, as the time extended, these alkoxyamine bonds were finally cleaved as discussed above.

In order to prove the mechanism, PS-*b*-(*c*-PHEMA) nanocapsules dispersed in PBS and ascorbic acid solution were degassed, purged with nitrogen (without oxygen), and stirred at 37 °C for 24 h. The result showed the size of the capsules did not change obviously, although the shell thickness and cross-link density decreased. This suggested that TEMPOH could not change back to TEMPO without oxygen, so the cross-linked bond could not be built again. But the carbon−carbon bonds were still cross-linked in this condition, which could maintain the morphology of nanospheres.

## ■ CONCLUSION

We have successfully synthesized a kind of novel intelligent polymeric nanocapsules by the surface-initiated atom transfer radical polymerization technique and atom transfer nitroxide radical coupling reaction, using alkoxyamine bonds as the cross-linkers and silica nanoparticles as the templates. Because PBS can accelerate the fragmentation reaction of the cross-linked bonds, while ascorbic acid can promote the addition reaction to form the cross-linked bonds, the as-obtained PS-*b*-(*c*-PHEMA) nanocapsules displayed unique responsive behaviors: When only PBS solution was present, these nanocapsules were decomposed into polymeric pieces at 37 °C, which self-assembled into nanocapsules again when ascorbic acid was added. When both PBS and ascorbic acid existed together, the


dx.doi.org/10.1021/ma500006j | *Macromolecules* 2014, 47, 1914−1921

nanocapsules merged into larger capsules. Both the nanocapsules and capsules were finally disassembled into polymeric pieces as the time extended. This special responsive behavior may find some potential applications in delivery systems used for biomaterials, self-healing materials, catalysts, etc.

## ■ ASSOCIATED CONTENT

### Supporting Information

TGA thermograms of the nanospheres and nanocapsules at different stages; TEM images of different sizes of nanocapsules, and $PS_4$-*b*-(*c*-PHEMA) nanocapsules responsive to PBS and ascorbic acid, and responsive to PBS without ascorbic acid. This material is available free of charge via the Internet at http://pubs.acs.org.

## ■ AUTHOR INFORMATION


### Corresponding Author

*E-mail: lmw@fudan.edu.cn (L.W.).


### Notes

The authors declare no competing financial interest.

## ■ ACKNOWLEDGMENTS

Financial support was received from the National Natural Science Foundation of China (Grants 51133001 and 21374018), National "863" Foundation, Science and Technology Foundation of Ministry of Education of China (20110071130002), and Science and Technology Foundation of Shanghai (12 nm0503600, 13JC1407800).

## ■ REFERENCES


(1) Lee, J. S.; Feijen, J. *J. Controlled Release* **2012**, *161* (2), 473−483.
(2) Morris, C. A.; Anderson, M. L.; Stroud, R. M.; Merzbacher, C. I.; Rolison, D. R. *Science* **1999**, *284* (5414), 622−624.
(3) Lomas, H.; Canton, I.; MacNeil, S.; Du, J.; Armes, S. P.; Ryan, A. J.; Lewis, A. L.; Battaglia, G. *Adv. Mater.* **2007**, *19* (23), 4238−4243.
(4) Kim, Y. H.; Tewari, M.; Pajerowski, J. D.; Cai, S. S.; Sen, S.; Williams, J.; Sirsi, S.; Lutz, G.; Discher, D. E. *J. Controlled Release* **2009**, *134* (2), 132−140.
(5) Discher, B. M.; Won, Y. Y.; Ege, D. S.; Lee, J. C. M.; Bates, F. S.; Discher, D. E.; Hammer, D. A. *Science* **1999**, *284* (5417), 1143−1146.
(6) Samadzadeh, M.; Boura, S. H.; Peikari, M.; Kasiriha, S. M.; Ashrafi, A. *Prog. Org. Coat.* **2010**, *68* (3), 159−164.
(7) Poe, S. L.; Kobaslija, M.; McQuade, D. T. *J. Am. Chem. Soc.* **2006**, *128* (49), 15586−15587.
(8) Zhang, L. F.; Eisenberg, A. *Science* **1995**, *268* (5218), 1728−1731.
(9) Donath, E.; Sukhorukov, G. B.; Caruso, F.; Davis, S. A.; Mohwald, H. *Angew. Chem., Int. Ed.* **1998**, *37* (16), 2202−2205.
(10) Emmerich, O.; Hugenberg, N.; Schmidt, M.; Sheiko, S. S.; Baumann, F.; Deubzer, B.; Weis, J.; Ebenhoch, J. *Adv. Mater.* **1999**, *11* (15), 1299−+.
(11) Wendland, M. S.; Zimmerman, S. C. *J. Am. Chem. Soc.* **1999**, *121* (6), 1389−1390.
(12) Wu, T.; Zhang, Y. F.; Wang, X. F.; Liu, S. Y. *Chem. Mater.* **2008**, *20* (1), 101−109.
(13) Mandal, T. K.; Fleming, M. S.; Walt, D. R. *Chem. Mater.* **2000**, *12* (11), 3481−3487.
(14) von Werne, T.; Patten, T. E. *J. Am. Chem. Soc.* **2001**, *123* (31), 7497−7505.
(15) Fu, G. D.; Shang, Z. H.; Hong, L.; Kang, E. T.; Neoh, K. G. *Macromolecules* **2005**, *38* (18), 7867−7871.
(16) Mu, B.; Liu, P. *React. Funct. Polym.* **2012**, *72* (12), 983−989.
(17) Liu, F. T.; Eisenberg, A. *J. Am. Chem. Soc.* **2003**, *125* (49), 15059−15064.
(18) Jiang, X. Z.; Luo, S. Z.; Steven, P. A.; Shi, W. F.; Liu, S. Y. *Macromolecules* **2006**, *39* (18), 5987−5994.
(19) Chu, L. Y.; Yamaguchi, T.; Nakao, S. *Adv. Mater.* **2002**, *14* (5), 386−389.
(20) Klaikherd, A.; Nagamani, C.; Thayumanavan, S. *J. Am. Chem. Soc.* **2009**, *131* (13), 4830−4838.
(21) Georgina, K. S.; Elvira, T.; Almar, P.; Angus, P. R. J.; Frank, C. *Nano Lett.* **2007**, *7* (6), 1706−1710.
(22) Suneel, B.; Margaret, B.; David, A. S. *Macromolecules* **2005**, *38* (22), 9216−9220.
(23) Rutger, J. I. K.; de Matthijs, G.; Gijs, J. M. H.; Cor, E. K.; Henning, M.; Andreas, H. *Macromolecules* **2010**, *43* (9), 4126−4132.
(24) Santosh, A.; Che, J. H.; Zhang, L. F. *ACS Nano* **2010**, *4* (1), 251−258.
(25) Stöber, W.; Fink, A.; Bohn, E. *J. Colloid Interface Sci.* **1968**, *26* (1), 62−69.
(26) Kurosaki, T.; Lee, K. W.; Okawara, M. *J. Polym. Sci., Part A: Polym. Chem.* **1972**, *10* (11), 3295−3310.
(27) Nicolay, R.; Marx, L.; Hemery, P.; Matyjaszewski, K. *Macromolecules* **2007**, *40* (26), 9217−9223.
(28) Jin, Y.; Zhang, L.; Zhang, M.; Chen, L.; Keung Cheung, P. C.; Oi, V. E. C.; Lin, Y. *Carbohydr. Res.* **2003**, *338* (14), 1517−1521.
(29) Save, M.; Granvorka, G.; Bernard, J.; Charleux, B.; Boissière, C.; Grosso, D.; Sanchez, C. *Macromol. Rapid Commun.* **2006**, *27* (6), 393−398.
(30) Zhang, Z. N.; Wang, G. W.; Huang, J. L. *J. Polym. Sci., Part A: Polym. Chem.* **2011**, *49* (13), 2811−2817.
(31) Paul, B.; Sylvain, R. A. M. *Chem. Commun.* **2011**, *47* (14), 4291−4293.
(32) Gérard, A.; Paul, B.; Sylvain, R. A. M.; Germain, O. *Polym. Chem.* **2012**, *3* (10), 2901−2908.
(33) Mikhail, Z.; Olga, B.; Chen, X.; Vladimir, B. G.; Laurent, B. *J. Polym. Sci., Part A: Polym. Chem.* **2012**, *50* (16), 3437−3443.
(34) Denis, B.; Didier, G.; Sylvain, R. A. M.; Paul, T. *Chem. Soc. Rev.* **2011**, *40* (5), 2189−2198.
(35) Warren, J. J.; Mayer, J. M. *J. Am. Chem. Soc.* **2010**, *132* (22), 7784−7793.
(36) Creutz, C. *Inorg. Chem.* **1981**, *20* (12), 4449−4452.
(37) Yang, H.; Chen, J. Q.; Li, J.; Lv, Y.; Gao, S. *Appl. Catal. A: Gen.* **2012**, *415*, 22−28.
(38) Zetterlund, P. B.; Nakamura, T.; Okubo, M. *Macromolecules* **2007**, *40* (24), 8663−8672.
(39) Nakamura, T.; Zetterlund, P. B.; Okubo, M. *Macromol. Rapid Commun.* **2006**, *27* (23), 2014−2018.
(40) Jauder, J.; Chiua, W. Y. *Polym. Int.* **2010**, *59* (12), 1639−1649.